

Full Paper: Commercial ficoll, rather heterogeneous in molecular weight but generally considered to be non-ionic, is demonstrated to contain negatively charged residues on about 50% of its macromolecular components. We have fractionated this material by size exclusion chromatography on Sephacryl S-400 HR (under non-adsorbing conditions) according to size and charge, taking advantage of the influence of ionic strength on elution. We subsequently applied the same strategy for physical characterization of some of these fractions on Superose-6. These

measurements illustrate a new chromatographic approach for estimating the charge and zeta-potential of macroionic solutes. We also consider the electro-osmotic swelling of Superose-6, and the possible implications of hydration and charge induction effects for the use of universal calibration. Lastly, we provide a detailed analysis of the sources of error in the measurement of retention volume in SEC and the related limitations with respect to the determination of apparent molecular size.

A Method for the Quantitation of Charge by Size Exclusion Chromatography Demonstrated with Components of Ficoll 400

Yuxin Zhu,¹ Martin Potschka,^{*2} Paul L. Dubin,^{*1} Chun-hua Cai¹

¹ Department of Chemistry, Indiana University-Purdue University, Indianapolis, USA 46202–3274

² Porzellangasse 19, A-1090, Vienna, Austria

Introduction

Solute retention in size exclusion chromatography (SEC)^[1,2] may be described by the chromatographic partition coefficient:

$$K_{\text{SEC}} = \frac{V_e - V_0}{V_t - V_0} \quad (1)$$

where V_e is the elution volume, V_0 is the void volume and V_t is the total column volume. Many models have been proposed to predict the dependence of the partition coefficient K_{SEC} on solute size.^[3–6] However, a universal definition for solute size is then required. Usually, the size is measured by the hydrodynamic effects of the solute, i.e. the viscosity radius (R_η). However, many researchers have also used the Stokes radius (R_s), obtained from the measured translational diffusion coefficient in conjunction with the Stokes-Einstein equation, or the radius of gyration (R_G), which is purely determined by the geometry of the solute. Theoretical treatments suggest the mean projection length (X) which is not amenable to direct experimental evaluation, but may be calculated for solutes of well-defined geometry. It may in fact be that none of these can serve as a universal parameter for solutes of all kinds of structures and shapes.^[7]

The chromatographic measurement of solute size is further complicated by charge effects that exist widely in aqueous SEC.^[8,9] Repulsive electrostatic interactions

between anionic SEC solutes and packings result in an apparent size for the solute larger than the size that is determined in bulk solution, and thus in general are not welcomed. The simplest way to eliminate electrostatic interactions is by increasing the ionic strength of the mobile phase. On the other hand, isoenzymes may be separated at low ionic strength due to differences in net charge^[9] and small amounts of contaminating charge in dextran preparations have been identified first by SEC.^[10] If retention in SEC depends on the solute charge, SEC could in principle be used to measure solute charge. This approach has not been well developed, perhaps because of the absence of a well-established theory for the dependence of K_{SEC} on charge, or perhaps because of a lack of calibration standards, i.e. small particles of known charge.

Charge effects in SEC have been summarized elsewhere.^[8,9] Booth and co-workers^[11] used the electrical double layer on the surface of latexes to explain their early elution on porous glass columns. This allowed them to rationalize the result that the elution volume, V_e , varied inversely with the square root of the ionic strength of the mobile phase, i.e. $V_e \sim I^{-1/2}$. Dubin et al.^[12,13] attributed ionic strength effects on the elution of sodium polystyrene sulfonate (also on porous glass columns) to a diminution of the effective pore volume due to the repulsive potential on the surface of the packing. A “repulsion

length", X_e , was used to measure the difference between the geometric pore radius and the apparent effective pore radius for a given solute. From either point of view, the elution volume depends on the volume that the solute has sampled on the way through a column. Smith and Deen^[14] proposed a theoretical model for charged cylindrical pore and spherical solutes, and calculated the electrical potential and hence the partition coefficient. Dubin compared experimental data for sodium polystyrene sulfonate on porous glass to Smith and Deen's calculation and found good agreement,^[15] later with dendrimers agreement was poor.^[16] Potschka gave an analysis of the electrostatic repulsion distances for packings with various surface geometries^[17] and experimentally showed a linear relationship between the apparent SEC size of proteins (R_{eff}) and the inverse square root of ionic strength of the mobile phase.^[9, 18, 19] Dubin and collaborators showed the same linearity for dendrimers.^[16] According to Potschka, R_{eff} can be viewed as a sum of the viscosity radius (accounting for shape) and the electrostatic repulsion length (accounting for charge).^[18] It should be noted that all the preceding works consider only a uniform charge solute distribution, so that effects of solute charge heterogeneity have been so far ignored.

Experimental studies of charge effects in SEC are best done using both solutes of well-defined shape and charge, and neutral solutes of known size as reference compounds. Charge, structure and shape are well established for many proteins. Neutral polysaccharides such as pullulan and dextran are often used as standards in aqueous SEC, but, as statistical chains, do not have unambiguous geometrical radii. Ficoll, another polysaccharide that is synthesized by cross-linking sucrose with epichlorhydrin, is of particular interest because it is highly branched and therefore relatively dense.^[20] It is presumed to be a porous sphere (ca. 15% solid)^[21] and is expected to maintain a constant geometrical size regardless of ionic strength of mobile phase. Because of these qualities, ficoll has been extensively used to probe the dimension of both physiological^[22] and synthetic^[20, 23] membranes. However, characterization data for ficoll are very limited. In this paper, we will show that commercially available ficoll in fact consists of species that carry charges of different amount. We demonstrate the use of SEC to quantitatively measure the amount of solute charge with a sensitivity beyond that of most other methods.

Experimental

Chromatography

A Superose-6 HR column was used for all analytical work. The set-up included a Minipump (Milton Roy, Riviera Beach, Florida), R401 Differential Refractive index detector (Waters Associate, Framingham, Massachusetts), a model

7010 injection valve (Rheodyne, California) and chart recorder. Pullulan standards (Showa Denko U.S.A., New York) were used to calibrate the column in pure water; in $I = 100$ mM, pH = 8.00 Tris/HCl buffer; and in $I = 3$ mM, pH = 2.7 phosphate buffer. Partial calibrations were also performed in other eluants. The column was equilibrated overnight with each buffer prior to injection. Typical lapse time between injections (usually 100 μ L) was 50 min. Chart recorder speed was usually 1 cm/min, calibrated to one part in 1000. All experiments were done at room temperature (about 23 °C). All injections were made with samples dissolved in the eluant, since it was found that other procedures affected elution, even for pullulan.

Nominal flow rates, chosen around 0.30–0.40 mL/min, were determined gravimetrically daily with a precision of 0.002 mL/min. Solutions of less than 10% D₂O in eluant were injected at least twice a day to monitor flow stability. The average drift of retention volumes during continuous pump operation on 15 selected days spanning a period of 10 months was $\pm 0.5\%$ and the largest individual datum was 1.5%. This flow rate drift was not correlated (based on Spearman-Brown-Wilcoxon rank correlation coefficient^[24]) to any experimental variables, such as the time interval used

Table 1. Reproducibility of experimental conditions^{a)}

Sample	Rel. deviation of retention volume (gravimetric) ^{b)}	Rel. deviation of retention volume (D ₂ O retention) ^{c)}	Mean retention volume (mL) ^{b)}
Condition: high ionic strength ^{d)}			
ficoll F17			12.99
Ficoll F17-9			13.02
Condition: medium ionic strength ^{e)}			
ficoll F17-6	$\pm 0.9\%$	$\pm 1.0\%$	10.42
ficoll F17-9	$\pm 2.0\%$	$\pm 0.7\%$	11.07
Ficoll F17-17	$\pm 1.1\%$	$\pm 1.8\%$	12.33
D ₂ O	$\pm 1.2\%$	p. d. zero	20.96
mean error	$\pm 1.3\%$	$\pm 1.2\%$	
Condition: low ionic strength ^{f)}			
ficoll F17-peak'6'	$\pm 2.1\%$	$\pm 3.3\%$	7.01
ficoll F17-peak'9'	$\pm 2.2\%$	$\pm 3.4\%$	8.04
ficoll F17-peak'17'	$\pm 1.1\%$	$\pm 2.4\%$	11.90
D ₂ O	$\pm 1.2\%$	p. d. zero	21.12
mean error	$\pm 1.6\%$	$\pm 3.0\%$	

^{a)} On the same Superose-6 column and equipment at a flow rate of 0.4 mL/min and room temperature with a recording accuracy of $\pm 0.1\%$ for 20 mL, increasing to $\pm 0.3\%$ at 7 mL retention.

^{b)} Based on occasional gravimetric calibration of flow rate.

^{c)} Two separate D₂O injections immediately preceding and following the samples were used to normalize flow rate via peak retention.

^{d)} In Tris/HClO + NaCl pH 8.0, $I = 100$ mM.

^{e)} 3 different experiments (at intervals of 2 months) in Tris/HCl pH 8.0, $I = 3$ mM.

^{f)} 2 different experiments (at an interval of 4 months) in Tris/HCl pH 8.0, $I = 0.3$ mM. A third experiment with matching D₂O values had to be excluded due to inconsistent results for all of the ficoll fractions.

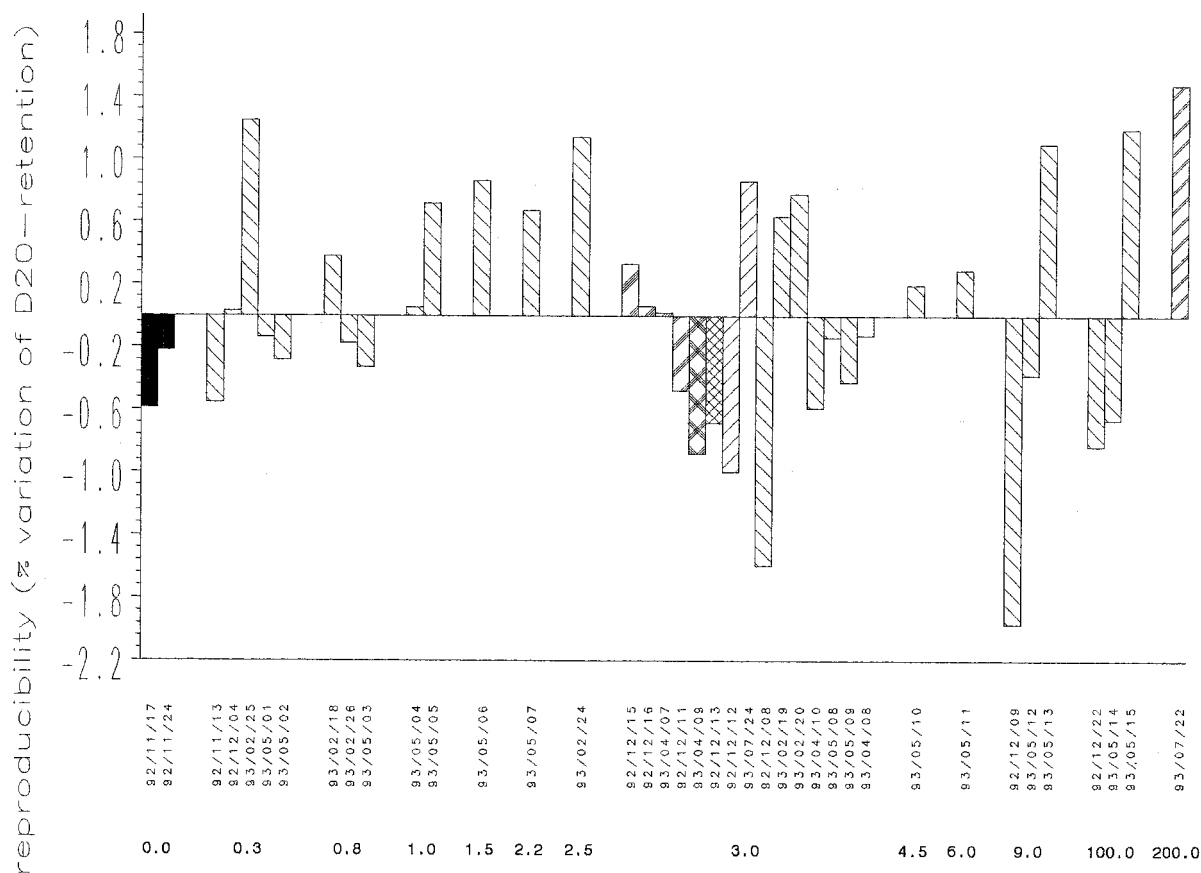


Figure 1. Reproducibility of D₂O elution in different sets of experiments (at days shown). The average daily D₂O retention (almost always the mean of at least two measurements early and late during the day plus a gravimetric calibration at some other time of the day) is presented as percent deviation from the overall mean of 21.05 mL. Data are blocked into groups of increasing ionic strength (from pure water on the left to I = 200 mM ionic strength to the right) with a unique symbol for each pH. The density of the pattern increases from pH 8.0 to pH 2.7 and the kinds of pattern are: (□) Tris-HCl, (□) Na-phosphate, (X) Na-acetate, (□) Na-carbonate pH 10, (■) pure water.

for measurement, the calendar date, or eluant composition. The mean flow rate reproducibility of interrupted, but gravimetrically calibrated, operation was $\pm 0.7\%$ for D₂O (see Figure 1) which is of the magnitude expected for combined flow rate drift and measurement error. The 95%-reliability of individual measurements is thus about $\pm 2\%$ in retention volume, which translates to less than 0.5 nm uncertainty in the apparent radius (see below), and is much smaller than the effects we observe. Tab. 1 shows that normalization to D₂O elution (using D₂O as a “marker”) does not improve the data.

A preparative-scale column (580 mm \times \varnothing 25 mm) (LDC/Milton Roy) was packed in our lab with Sephacryl s-400 HR gel (Pharmacia, Piscataway, New Jersey). The column efficiency was about 5000 plates/meter, as determined by injection of D₂O at a flow rate of 1.2 mL/min. An automatic sample collector and sample injection/loading device along with the controlling circuits were designed and constructed in our lab. An R401 differential refractive index detector (Waters Associate, Framingham, MA) was installed to monitor the chromatogram and the operation of injector and fraction collector (a mark is recorded for each step motion of the frac-

tion collector and each injection). The flow rate for most cases was 4 mL/min.

Eluants

Mobile phase buffers were freshly made from analytical grade chemicals and deionized water, and were degassed before use. The pH and ionic strength of the buffers were calculated based on the data in ref.^[25] in combination with Davies\9 form of the Debye-Hückel equation to calculate the pK for each particular ionic strength.^[25] This was verified by pH measurements (\varnothing pH meter, Beckman, Fullerton, CA). The reproducibility of eluant composition was $\Delta pH < \pm 0.05$ and $\Delta I < \pm 10\%$. The following types of buffers were used: phosphate for pH 2.7, 4.0, 4.5, 7.0; acetate for pH 4.0, 5.0; carbonate for pH 10; Tris/HCl for pH 8.0; NaCl was used only at pH 8.0 and only to raise the ionic strength above 6 mM. Sodium (and Tris) based buffers were used throughout this study, albeit potassium buffers have occasionally been used earlier without apparent difference. Buffers were prepared fresh with degassed water in quantities of some 5 L by weighting solid salts to final specifications whenever pos-

sible. pH was, however, measured as the control. To calculate the Debye-Hückel parameter κ we used $\kappa = 3.3 I^{1/2} \text{ nm}^{-1}$.

Materials

Ficoll 400 (molecular weight of 400,000 g/mol) was purchased from Pharmacia. Pullulan standards were from Showa Denko. Ovalbumin was from Sigma (A5503). Myoglobin (horse) was from CalBiochem (47592); and β -lactoglobulin (bovine milk) was from Sigma (L-2506).

Fractionation

Fractionation of ficoll 400 was performed by repeated injections on a Sephacryl s-400 HR column in 0.1 M NaOH mobile phase at a flow rate of 4 mL/min. The mobile phase was chosen to suppress the electrostatic interaction and to prevent aggregation. Ficoll 400 was dissolved in the mobile phase at a concentration of 20 mg/mL, sonicated for about 5 h to eliminate any possible aggregation, and filtered through a 0.20 mm filter (Scientific Resources Inc., NJ). The fractions were combined, dialyzed, lyophilized and weighed.

Electrophoretic Light Scattering

Electrophoretic light scattering was performed on a Coulter (Hialeah, FL) DELSA 440 at 25 °C at scattering angles of 8.6°, 17.1°, 25.6° and 34.2° in pH 8.0 Tris/HCl buffer, at an ionic strength of 0.3 mM. Thus, in our experiments, the Debye-Hückel parameter was $\kappa = 0.057 \text{ nm}^{-1}$. The solution viscosity was $\eta = 0.89 \text{ cP}$. The electric field was applied at currents of 0.25 mA and 0.3 mA. The principle of electrophoretic light scattering is that charged particle will move in a applied electrical field; the velocity of the motion depends on the amount of charge, the size of the particle, the viscosity of the solution, and on the ion atmosphere which screens the particle from the full effect of the external field. The velocity of the motion can be detected by the Doppler effect from light scattering.^[26] The mobility u is defined as velocity of the particle under unit electrical field. Detailed descriptions of electrophoretic light scattering can be found in ref.^[27-29] From the measured mobility u , the charge on particles can be calculated. In the case of dense spherical particles with isotropic surface charge we have the following relation:^[28]

$$Q = (6 \pi / e) \eta u a \{ (1 + \kappa a) / H(\kappa a) \} \quad (2)$$

where Q is the netcharge on particle, e is the electronic charge, a is the radius of particle (in nm), η is the viscosity of the solution (in cP), u is the electrophoretic mobility (in $\mu\text{m} \cdot \text{cm} \cdot \text{V}^{-1} \cdot \text{sec}^{-1}$), κ is the Debye-Hückel constant, and the numerical factor $6 \pi / e$ is 1.177 in the appropriate units. $H(\kappa a)$ is Henry's function, a complicated function whose numerical value is always between 1.0 and 1.5, but is quite close to unity under our experimental conditions.^[30] Henry's function accounts for the modifications of the viscous flow of the solvent past the moving particle due to its surrounding ion atmosphere. The role this ion atmosphere plays in screening the electric field is expressed with $(1 + \kappa a)$, viz. the

Debye-Hückel approximation for low ionic strength. For colloid systems, the net charge Q is often expressed in terms of the zeta potential

$$\zeta = e \kappa T Q / (1 + \kappa a) \quad (3)$$

Equation (3) may be used to translate the reported net charges into zeta potentials.

Results and discussion

Column Calibration

A prime concern in studies that rely on comparisons between different eluant conditions is matrix rigidity. We used D₂O to measure total column liquid volume V_t for all eluants (Figure 1) and performed a variety of statistical correlation tests. We found no correlation with pH, ionic strength or other experimental variables. In all likelihood, the solid part of the matrix polymer itself does not swell at all (this is an aspect different from that of rigidity and swellability of the overall porous structure) and V_t remains invariant. The observed variation thus can be entirely attributed to pump instability and consequently can be used to estimate the limits of analysis for other solute sizes as well.

Pullulan P800 was used to determine V_0 , i.e. the liquid volume surrounding the matrix beads outside of its pores. At pH 2.7, where the gel is largely neutralized, V_0 and the entire calibration graph are essentially identical to the results obtained at high I and pH 8.0 where residual matrix ionophores are fully dissociated but the electrostatic interactions are largely screened. With decreasing I , the calibration curve shifts towards lower V_e in proportion to the degree of non-screened surface charge density. Calibration curves for pure water and for pH 8.0, $I = 0.8 \text{ mM}$ are essentially identical, while elution at pH 8.0, $I = 3 \text{ mM}$ is intermediate as is true for all other eluants that are not shown in Figure 2. While we cannot exclude the possibility of small electrostatic repulsion effects arising from mirror charges^[9] even for non-ionic polymers like pullulan in response to charges on the matrix (explicit calculation of this effect has been provided^[14]), we consider it more likely that the self-repulsion of the charged matrix leads to reversible swelling of the pores. Under high packing density, this leads to bead deformation with the larger pores becoming compressed, while the overall liquid volume inside the beads, i.e. $V_t - V_0$, increases (see Figure 2 and its insert).

Extending an earlier suggestion^[31] we found that excellent fit of the calibration curves for Superose-6 may be obtained with an expression based on a model of the stationary phase comprised of equal numbers of cylindrical pores of all sizes up to an arbitrary maximum. Thus the volumetric calibration curve function becomes

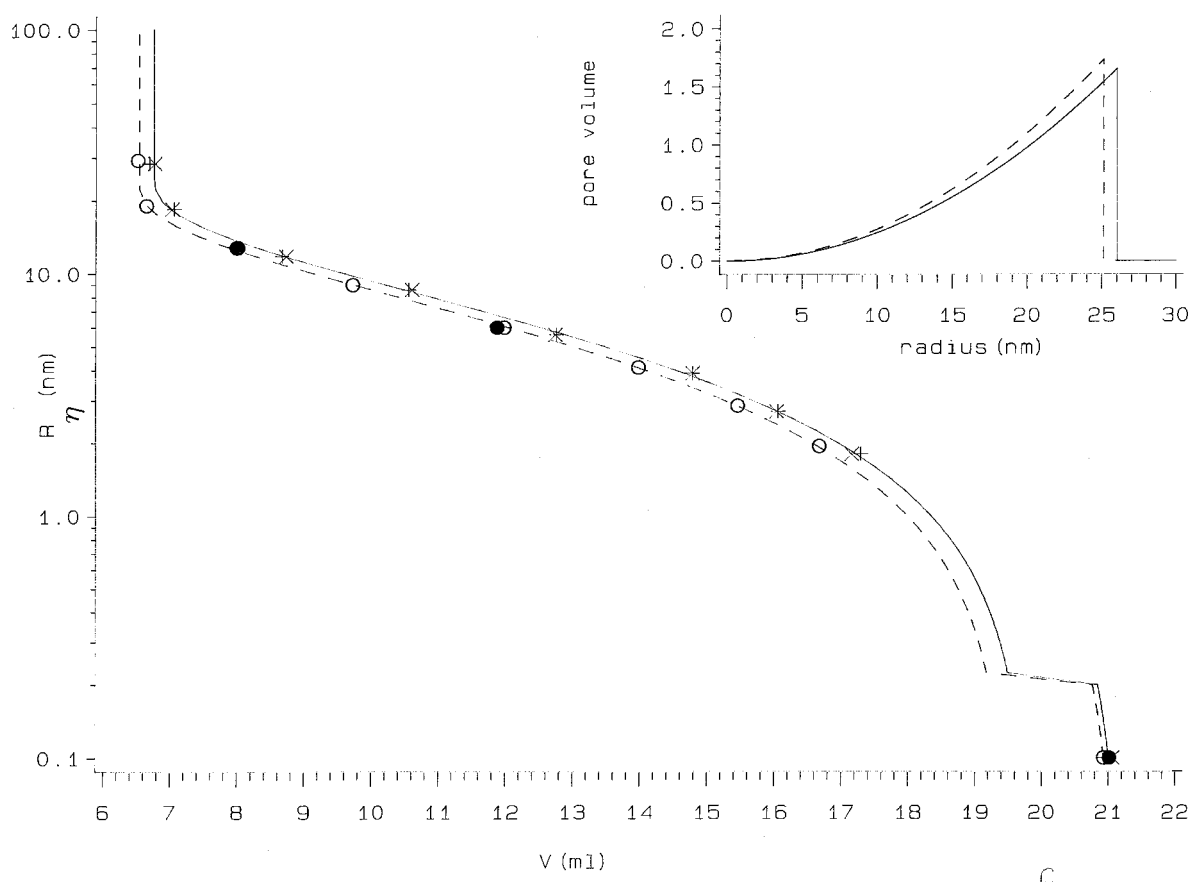


Figure 2. Pullulan calibration curve for Superose-6 in: (+) Tris/HCl plus NaCl buffer, $I = 100$ mM, pH = 8.00; (x) phosphate buffer, $I = 3$ mM, pH = 2.70; (●) Tris/HCl buffer, $I = 0.8$ mM, pH = 8.00; (o) pure water. These conditions represent the extremes of calibration within the range of our conditions; (—) low electro-osmotic pressure, (---) high electro-osmotic pressure. The calibration model is described in the text. Reported volumes include all extra-column liquid from the injection valve to the detector cell. Insert: pore volume distribution derived from our model for the stated extremes of swelling (—, ---).

$$V_e = V_0 + \frac{V_e - V_0}{3R_{\max}^2} \int_{R_\eta + R'}^{R_{\max}} r^2 \left(1 - \frac{R_\eta + R'}{r}\right)^2 dr \quad (4)$$

where the values of V_0 , V_t , R_{\max} and R' are derived from a simultaneous least squares fit of the pullulan data, with the corresponding values: $V_0 = 6.62 \pm 0.15$ mL, $V_t = 21.21$ mL, $R_{\max} = 25.5 \pm 0.5$ nm, and $R' = 0.9 \pm 0.2$ nm, depending on the eluant (see Figure 2). Since the values for V_0 and V_t depend on the fill length of the column and the extra-column tubing, they may differ between various laboratory setups. The integration is performed only over those values of r corresponding to pores sizes large enough for the solute to enter. The resulting pore volume distribution function is shown in the insert of Figure 2. R_η values were based on intrinsic viscosities of pullulan measured in water^[15] and in 200 mM phosphate buffer,^[32,33] which are nearly identical.

R' is an adjustable parameter that can be interpreted in two ways. Taken literally as implied by Equation (4) it expresses the difference between the viscosity radius

(sometimes, somewhat ambiguously, called the equivalent hydrodynamic radius^[34]) and the radius (undefined) that controls SEC, which we might refer to as R_{SEC} . The exact nature of R_{SEC} is the subject of numerous investigations and is not the primary goal of this study; but if Equation (4) is correct, R_{SEC} exceeds R_η by ca. 0.9 nm even for small solutes. This coincides with molecular dynamics simulations of low molecular weight oligomers in cylindrical cavities that claim retention radii to be larger than R_η in principle.^[35] Alternatively, and indistinguishably at this point, one may imagine that deviations between the data and the simple geometric model arise from the presence of micropores accessible to water but not to the solutes, a view readily visualized by a difference between the apparent elution volume extrapolated to low MW from the pullulan curve in Figure 2 and the measured V_t for D_2O . Mathematically it means transformation of Equation (4) into separate integral terms for R_η and R' . R' may well turn out to be a combination of both effects whose separation depends on independent evidence.

In our fits we obtained figures of merit that are as good as possible with our current flow rate accuracy: $\pm 0.7\%$ for pullulan retention volumes in moderate I buffer, and $\pm 0.5\%$ in water. Calibration curves for the two conditions themselves differ by up to 8% in retention volume (see Figure 2).

Once the four calibration parameters (V_0 , V_t , R_{\max} and R') are known, any retention volume can be converted to its hydrodynamic radius via Equation (4) (Figure 2). While this is often done with recourse to a single calibration curve, better results are obtained if one uses the calibration curve relevant to the eluant in question. Lacking complete calibration information for all of the eluants, we used the pH variation of ficoll fractions F17-6 and F17-9 (see below) to identify eluants of equivalent electro-osmotic force, and interpolated the calibration of Figure 2 accordingly (at $I = 3$ mM and in the range of pH 2.7–6.4 we used $[I(M)^{-1/2}]_{\text{equiv.}} = 4 \text{ pH} - 6.8$).

Chromatogram of Ficoll Fractions

Twenty fractions of ficoll 400 with apparent radii of 2.3 nm to 16 nm were obtained in amounts from 20 mg to 120 mg. Analysis on Superose-6 in $I = 100$ mM, pH = 8.00 Tris buffer showed the polydispersities to be around 1.1. The chromatogram of a typical fraction (F17) in this buffer is shown in Figure 3a along with the chromatogram in $I = 0.3$ mM, pH = 8.00 Tris buffer (Figure 3b). The surprising peak multiplicity in the later could be explained if the fractions contained some charge. In 100 mM buffer, the charge effects would be suppressed, but in the low ionic strength buffer, repulsive interactions between solute and packing could influence the elution. The presence of a multiple peak instead of a very broad chromatogram indicates that the degrees of charge are so small that a wide variety of charge states does not exist. While there is no obvious mechanism for the incorporation of charge groups in ficoll synthesis, we hypothesize that the peaks labeled p17, p9, and p6 in Figure 3b correspond to a neutral species, weakly charged species and a more highly charged one respectively (a fourth component might not be fully resolvable). Note that under conditions of Figure 3a, component p6 has an identical elution volume to the single peak in Figure 3a. The phenomenon of a single peak in high ionic strength buffer and multiple-peaks in low ionic strength buffer was observed for various ficoll samples that we tested, including ficoll 70.

Isolation of Charged Ficoll

Fraction F17 was further fractionated in $I = 0.3$ mM, pH = 8.00 Tris buffer to produce sub-fractions. We presume that these species are about the same molecular size but separate under these SEC conditions according to the

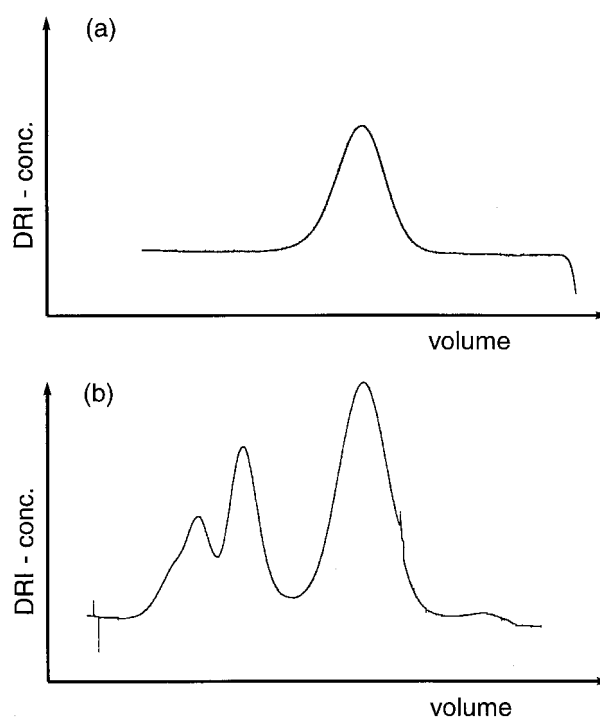


Figure 3. SEC chromatogram of ficoll 400 K-fraction F17 measured at pH = 8.0 in: (a) high ionic strength Tris/HCl plus NaCl buffer ($I = 100$ mM) on Superose-6, and (b) in extra low ionic strength Tris/HCl buffer ($I = 0.5$ mM) on Sephacryl s-400 HR.

amount of charges they carry. The fractionation was performed on Sephacryl s-400 HR in the same condition as the initial fractionation of ficoll 400 except for the buffer. The sub-fractions were dialyzed, lyophilized and weighed. The three isolated sub-fractions that were studied further are denoted as F17-17, F17-9 and F17-6. These exhibited the same elution volumes as the respective peak maxima in the starting material F17 (see Figure 3). For convenience we have labeled these maxima p6, p9 and p17, respectively. At high ionic strength, the isolated fractions eluted identically (see Tab. 1). Material accumulated from the valley (sub fractions 12/13) behaved almost like F17-9, which demonstrates the absence of species of intermediate charge (data not shown).

These fractions were tested by electrophoretic light scattering (ELS). In this measurement also, each fraction appeared to be rather homogeneous with respect to charge. F17-17 proved to be neutral, F17-9 is weakly charged and F17-6 is somewhat more charged. We measured electrophoretic mobilities of $-1.4 \pm 0.1 \mu\text{m} \cdot \text{cm} \cdot \text{V}^{-1} \cdot \text{sec}^{-1}$ for F17-9, and $-2.2 \pm 0.1 \mu\text{m} \cdot \text{cm} \cdot \text{V}^{-1} \cdot \text{sec}^{-1}$ for F17-6. We may apply Equation (2) and obtain apparent values of $Q/a = -1.5$ and -2.3 , respectively, but it is necessary to recognize that the mobility of individual polymer segments in ficoll tends to preclude the model of a surface-charged sphere. Thus, it is impossible at present

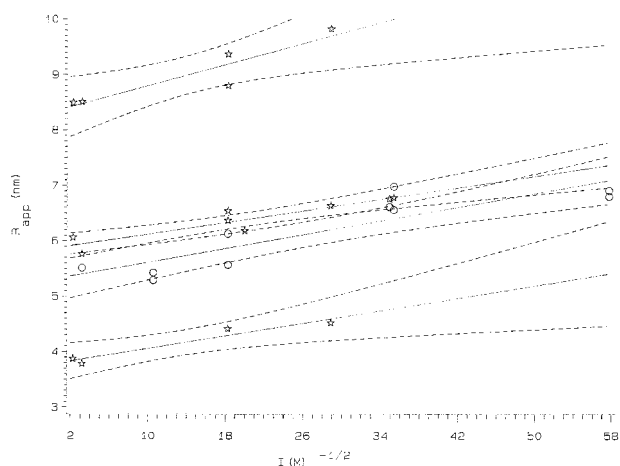


Figure 4. Effects of eluant variation for non-electrolytes (basis: single reference calibration of pullulan at high ionic strength). (○) ficoll F 17-17 at pH 7.0 or pH 8.0 (varying ionic strength); (☆) pullulan (p20), p 50, p 100) at pH 7.0 or pH 8.0 (varying ionic strength) and at pH 4.5 (high ionic strength). The slopes in part reflect the swelling of the matrix, a feature also expressed in Figure 2 and 8. (—) non-weighted linear regression through corresponding data points; (---) 3σ (95%) – confidence limits of fit.

to report unambiguously the numerical values of the net charge obtained by this method. However, there can be no doubt that ficoll F17-6 and F17-9 are charged, and that the former is more highly charged than the latter.

SEC Analysis of Non-ionic Ficoll F17-17

It has been generally assumed in previous applications of universal calibration that the elution of neutral polymers is ionic-strength-independent. The current results suggest that comparisons between retention volumes obtained in different eluants of different ionic strength may be more problematic than previously thought, although potential difficulties might be diminished on packings more rigid than Superose-6. Previous studies on charged macromolecules^[9] assumed that the matrix behaves ideally, and calculated R_{eff} values at different ionic strengths by reference to a single base calibration curve obtained with these solutes at high I . The present findings suggest that this approach is not rigorously correct. In fact, the application of this approach to pullulan yields distinct slopes (see Figure 4) which are now viewed as primarily consequences of changes in the stationary phase. Interestingly, the effect appears larger for ficoll F17-17 (which electrophoretic light scattering shows to be uncharged). Theory predicts that a dense non-ionic polymer should exhibit larger “mirror-charge” effects than a coiled polymer which does not exclude the necessary counterions from solvent locations within its equivalent sphere region (see ref.^[9, 14]). However, the isolated quantity of this sub-fraction

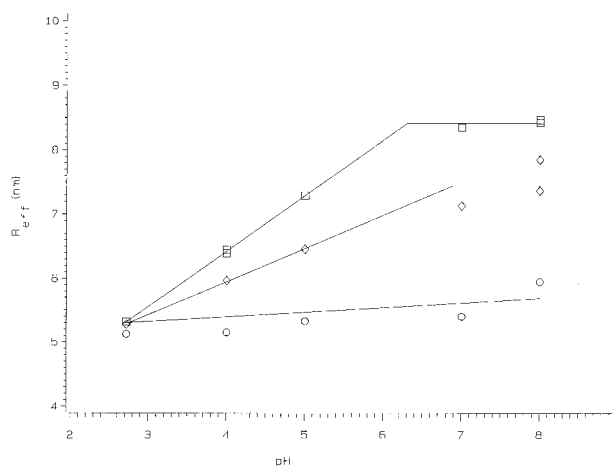


Figure 5. Dependence of effective elution radii (basis: interpolated pullulan calibrations) on mobile phase pH, in $I = 3$ mM buffer. (○) ficoll F 17-17; (◇) ficoll F 17-9; (□) ficoll F 17-6. The linear regression for F 17-17 was calculated from data of all ionic strengths properly scaled, the other lines are hand-drawn to guide the eye.

tion precluded precise viscometry, without which further interpretation of this point would be speculative.

Effects of pH

The dependence of the elution volume on pH for F17-17, F17-9 and F17-6 is shown in Figure 5, where the apparent size R_{eff} is plotted against the pH of the mobile phase at constant ionic strength of 3.0 mM. Since the surface charge increases with pH due to the presence of carboxylic groups on the gel,^[8] charge repulsion effects should lead to a diminution in V_e (and hence an increase in R_{eff}) with pH. At low pH, the R_{eff} values for F17-6 (p6), F17-9 (p9), and F17-17 (p17) converge because of the elimination of charge on the packing (and perhaps the solute as well). With increasing pH and charge, the effects rise to a plateau around pH 8. What appears to be a retarded elution of F17-17 at low pH (Figure 5) is within the experimental error of the data. The nearly pH-independent behavior of p17 (Fraction 17-17) is consistent with its neutrality deduced from ELS. As expected, the effect of pH on R_{eff} is larger for F17-6 than for the less charged F17-9.

Effects of Ionic Strength

The elution volume of the three sub-fractions F17-17, F17-9 and F17-6 is plotted as a function of the Debye-Hückel parameter, which is proportional to the ionic strength in pH = 8.00 mobile phase in Figure 6. For purpose of comparison, we choose solutes of known charge and size, the globular proteins ovalbumin, myoglobin and β -lactoglobulin. The ionic strength varies from 0.3 mM to

Table 2. Physical parameters for ficoll fractions and proteins

Sample	Net charge Q at pH 8.0, 25 °C			pI	Stokes radius (R_s /nm)	Chromatographic size (R_{eff} /nm) ^{a)}		Reduced screening length $dR_{eff}/d\kappa^{-1}$
	inferred (see text)	Electrophoretic	Titration			100 mM	2 mM	
ficoll F17-17	0	–	–	–	–	5.3 ± 0.1	5.6 ± 0.2	0.05 ± 0.01
ficoll F17-9	–1	–	–	–	–	5.4 ± 0.2	7.9 ± 0.3	0.43 ± 0.02
ficoll F17-6	–2	–	–	–	–	5.2 ± 0.4	9.2 ± 0.5	0.68 ± 0.04
myoglobin(horse)	–	–	$-1.3 \pm 0.5^{b)}$	$7.4^{b)}$	$1.91^{b)}$	2.1 ± 0.2	5.5 ± 0.3	0.57 ± 0.04
ovalbumin	–	$-14 \pm 2^{b)}$	$-16 \pm 2^{b)}$	$4.7^{b)}$	$2.96^{b)}$	3.6 ± 0.3	15.8 ± 0.7	2.08 ± 0.08
β -lactoglobulin ^{c)}	–	$-15 \pm 2^{b)}$	$-15 \pm 2^{b)}$	$5.2\text{--}5.4^{b)}$	$3.1^{d)}$	2.9 ± 0.4	13.1 ± 0.8	1.74 ± 0.09
					$2.89 \pm 0.05^{e)}$			

a) Apparent solute size in pH 8.0 buffer, based on retention relative to standard pullulan curves.

b) For details see Appendix.

c) Monomer below pH 3.0, dimer above pH 3.7; denatures above pH 9.4. The dimer exists in 3 distinct conformations with transitions at pH 5.1 and at pH 7--7.5.

d) For the high pH dimer conformation at pH 8.0; for details see Appendix.

e) Average value for the two dimer forms below pH 7.0; for details see Appendix.

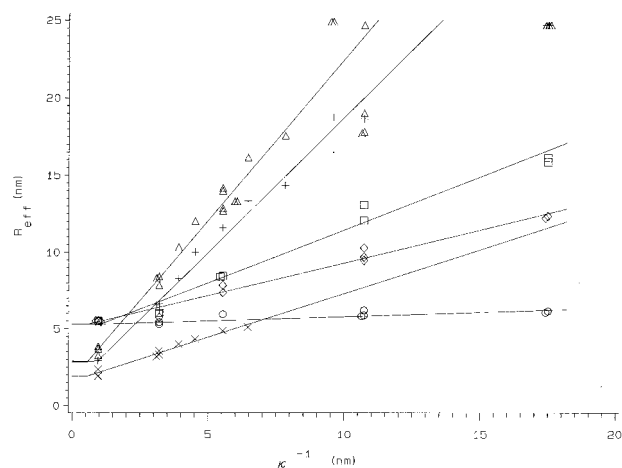


Figure 6. Effective elution radii (basis: interpolated pullulan calibrations) as a function of Debye-Hückel screening length ($\kappa = 3.3 I^{+1/2} \text{ nm}^{-1}$), in pH 8.0 Tris/HCl buffer. (o) ficoll F 17-17; (\diamond) ficoll F 17-9; (\square) ficoll F 17-6; (x) horse myoglobin; (+) β -lactoglobulin; (Δ) ovalbumin. Linear regressions were calculated with a 2% flow rate uncertainty (as shown in Figure 8) as the best-linear-unbiased-estimator for the weights and were limited to $R_{eff} < 17 \text{ nm}$. The regression for F 17-17 included data of all ionic strengths properly scaled.

100 mM. A linear relationship between apparent elution size and the inverse square root of the ionic strength of the mobile phase (expressed as κ^{-1}) was observed for all the sub-fractions, and also for the proteins up to the limit suitable for analysis ($R_{eff} < 17 \text{ nm}$). In general, the larger the amount of charge, the larger the slope of the line. The values of the slopes obtained in this study are presented in Table 2. This table also includes consolidated reference data for the three proteins myoglobin (horse), ovalbumin and β -lactoglobulin based on a critical review of the available literature^[36–59] (details are deferred to the appendix).

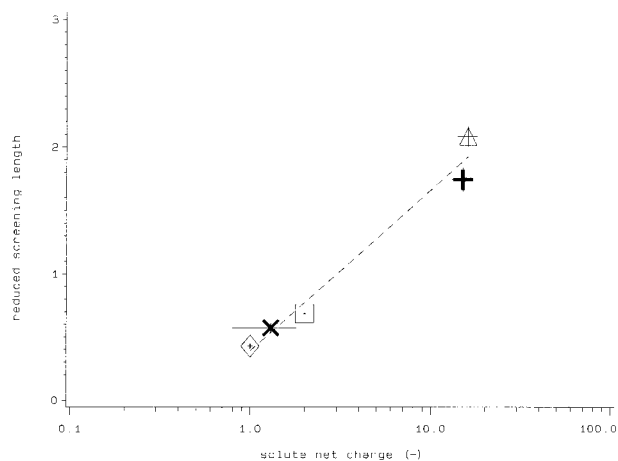


Figure 7. Correlation of reduced screening length with net charge. (\diamond) ficoll F 17-9; (\square) ficoll F 17-6; (X) horse myoglobin; (+) β -lactoglobulin; (Δ) ovalbumin. (–) 1σ -error bars. (– –) empirical regression line.

β -lactoglobulin possesses an extremely asymmetric charge distribution and binds to cation-exchange columns more strongly than ovalbumin^[42] even though the net charge of ovalbumin is higher or at least identical at pH 8.0. In comparison it can be seen from Figure 7 that the slope measured by SEC (to be identified as reduced screening length below) is approximately proportional to average net charge. A second order influence of charge patches on the reduced screening length cannot be excluded on the basis of the current comparison of only two proteins.

According to Potschka^[19] the slope x ($x = dR_{eff}/d\kappa^{-1}$) is the dimensionless reduced screening length. Multiplied with the Debye-Hückel parameter κ^{-1} (nm) for a particular eluant it yields the average electrostatic repulsion dis-

tance at equilibrium. It depends on the matrix charge, the charge of the solute and its geometric size (see also ref.^[60]). From ref.^[18] Equation (16) we get

$$\psi f \propto e^{+x} \quad (5)$$

ψ represents the surface potential (more precisely its pseudo potential^[17]) and f the geometry of interaction; it is presumed that the matrix remains at identical degrees of ionization and ion-binding. Then from ref.^[18] Equation (25) we approximate

$$f \propto R_s \quad (6)$$

We know that in the Debye-Hückel limit the surface potential is (see, e.g., Equation (19) of ref.^[61])

$$\psi = \kappa^{-1} (\kappa^{-1} + R_s)^{-1} (QR_s) \propto (QR_s) \quad (7)$$

where Q is the net charge of the spherical solute of radius R_s . We therefore expect that the reduced screening length primarily depends on net charge Q as long as Q is not too large:

$$x \propto \ln |Q| \quad (8)$$

and that particle size then amounts to a second order correction only. Comprehensive computations confirm the conclusions of the presented argument (see Figure 6 and 7 of ref.^[17]). Figure 7 (of the present paper) demonstrates this relationship empirically and furthermore stipulates that the ficoll charges are indeed as small as $Q = -1$ for F17-9 and $Q = -2$ for F17-6. It furthermore demonstrates that the chromatographic method is exquisitely sensitive to measure even small amounts of net charge.

In previous studies, the apparent size of proteins was found to vary linearly with $I^{-1/2}$ under conditions of electrostatic repulsion between solute and gel, finally reaching an apparent size independent of I .^[9, 32, 39] For a variety of proteins, this apparent size closely correlates with Stokes' radii and was observed at $I > 0.1$ – 0.2 M, regardless of net protein charge. Similar behavior is observed in the present case inasmuch as the curves for the ionic strength dependence of the pullulan-calibrated R_{eff} values converge upon the known geometric size at about $I = 100$ mM.

We assume that the several charge variants of ficoll F17, which elute identically at $I = 100$ mM in either pH 8.0 or pH 13.0 buffer, are all of equal mean geometric size, i.e. $R_s = 5.3$ nm (which based on Mark Houwink coefficients^[16] translates into some 81 K molecular mass). Their effective radii thus converge at rather moderate ionic strength. Likewise, two proteins, ovalbumin and thyroglobulin reached a limiting retention value at some moderate, common ionic strength regardless of pH (hence, net charge). The most likely explanation for this observation is as follows. The interaction between two charged species (solute and pore wall) depends on the

wall surface potential ψ via Equation (7). At high I , κ^{-1} becomes smaller than R_s and ψ decreases strongly. Consequently, a Debye length of 1 nm may be small enough to make the repulsive potential nearly negligible for a 5 nm sphere, if Q is not large.

The influence of electrostatic surface potential may also be suppressed by the presence of a non-electrostatic repulsion. One such effect has been called the hydration force and effects over a distance of 1–2 nm have been demonstrated by direct force measurements.^[62, 63] It is easily calculated from $R' = (dR_{\text{eff}}/d\kappa^{-1})\kappa^{-1}$ that at the mentioned points of convergence in Figure 6, the corresponding value for R' is 0.5–1.5 nm, which is in the range of such presumptive hydration forces. This interpretation implies that true chromatographic radii are always larger than geometric sizes by this amount. However, as long as all candidate solutes exhibit the same magnitude of hydration force, such a systematic difference would only be noted in relation to absolute pore dimensions derived from other techniques (such as porosimetry, electron microscopy or hydraulics).^[64]

Technical Performance

Exploring the limits of the method we identified three sources of error: pump instability, electro-osmotic swelling of the gels, and accuracy of buffer preparation.

Figure 8 presents the 95%-confidence limits of R_{eff} that are to be expected if pump instability (probed by D₂O retention) were the only source of error. It can be seen from Figure 8, as well as from Figure 4, that the pullulans, ficoll F17-17 and myoglobin all fall within this margin and errors are essentially dominated by flow instability. Our performance is quite comparable to other equipment and investigations^[39, 65, 66] and future technology would have to produce at least a fourfold improvement in order that flow rate instability not be the limiting technique factor. As it is unlikely that the mechanics of pump design could be substantially improved, performance will have to be advanced either with a flow feedback system^[67] or simply by replacing the fixed time base in current chromatography with accurate monitoring of actual volume flow.

Figure 8 also shows the propagated error of matrix instability. Quite robust results are obtainable in the crudest form of routine operation. The reduced screening length, whose evaluation is one of the principal physicochemical aims in this line of research is derived at quite acceptable levels of accuracy even upon full neglect of matrix instability (at least with Superose-6). With a fixed single reference calibration we obtain a value of 2.20 for ovalbumin instead of 2.08 (see Table 2), a quite minor systematic error. Similarly we find 0.61 instead of 0.57 for myoglobin, and 0.11 vs. 0.05 for ficoll F17-17. The extent to which our interpolation strategy for calibration was able to correct for matrix instability can be estimated as fol-

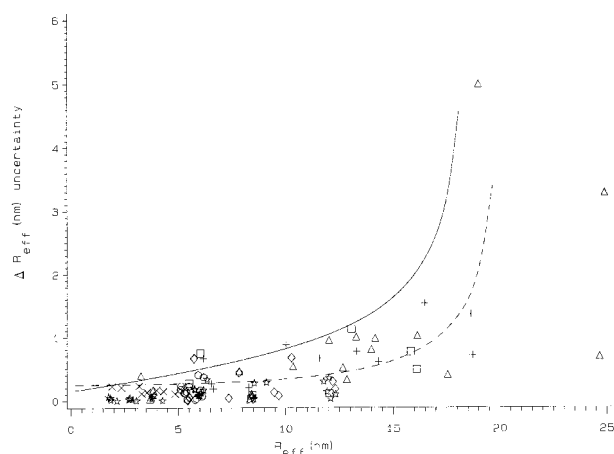


Figure 8. Reliability of SEC based size analysis. Shown are the values of the Superose-6 column derived from Figure 2, for missing values the uncertainty is infinitely large. (—) maximum possible error if variation of calibration graphs, which occurs when eluants deform the matrix to different extent, is not taken into account at all; (---) 3σ (95%) – confidence limit due to a 2% ($1\sigma = 0.7\%$) flow rate instability. Experimental residuals from best weighted linear regression (basis: multiply interpolated pullulan calibration) as shown in Figure 6: (o) ficoll F 17-17; (◊) ficoll F 17-9; (◻) ficoll F 17-6; (x) horse myoglobin; (+) β -lactoglobulin; (Δ) ovalbumin; (\star) pullulan of various sizes.

lows: The superposition of pump and matrix instability will be most significant for large R_{eff} close to V_0 . Then the dashed curve of Figure 8 alone is bound to underestimate the experimental uncertainty. Observing that reliability is truncated to $R_{\text{eff}} < 17$ nm implies that our interpolation strategy for calibration was still subject to some extra 2% of unaccounted matrix instability compared to 8% (Figure 2) in the case of total neglect. A detailed assessment of matrix rigidity and reproducibility is prohibitive at current performance levels but is within future reach.

Matrix instability, however, can only explain the larger scatter observed for the largest R_{eff} values. The dismal 10% level of standard deviation for R_{eff} in Tab. 2 is a direct consequence of yet a third source of error. Figure 8 shows that whereas results for pullulan, ficoll F17-17 and myoglobin are within the 2% margin attributable to flow rate error, the data for polyelectrolytes with large reduced screening length, i. e. large slopes in Figure 6, are not. For these solutes the error is believed to be dominated by inaccuracy in buffer ionic strengths. As confirmation, it can be seen from Figure 6 that the residuals of different solutes that have been analyzed with the same buffer lot are highly correlated. The propagated errors presumably are typical and representative of average equipment and care, as in the present work, but optimized wet chemistry techniques are likely to achieve a tenfold increase in ionic strength accuracy. With such improvements, chromatography may be extended to novel applications in the field of physical polymer analysis.

Conclusion

Commercial ficoll contains charged components which can be separated from uncharged material by chromatography in a mobile phase of sufficiently low ionic strength (I). A fraction isolated from ficoll 400 at high I is homogeneous with respect to molecular size but not with respect to charge. The diminution of retention times upon decrease in I furthermore offers a way to assess the degree of charge of the subfractions. This evaluation is based on the observed linearity of R_{eff} with I , and the dependence of $dR_{\text{eff}}/d\kappa^{-1}$ on solute charge. When globular proteins are used to “calibrate” this second relationship, estimates of one and two charges are obtained for the isolated subfractions of ficoll. It thus appears that proper calibration of a column with a series of standards of known charge and size leads to a useful method for estimating the charge of macroionic solutes. This method is in principle very sensitive, precise, and fast and requires only a very small amount of samples.

Appendix: Physico-Chemical Reference Data

Table 2 includes consolidated reference data for the three proteins myoglobin (horse), ovalbumin and β -lactoglobulin based on a critical review of the available literature as follows:

Myoglobin (horse):

net charge Q at pH 8.0, 25 °C (titration) = -1.3 ± 0.5 ; from similar myoglobin variants and derivatives^[36, 37] adjusted to $pI = 7.4$.

$pI = 7.4$; at room temperature.^[38]

Stokes radius (R_s /nm) = 1.91; quoted by ref.^[39]

Ovalbumin:

net charge Q at pH 8.0, 25 °C (electrophoretic) = -14 ± 2 ; based on measurements by Longworth^[40] a mobility of $-0.6 \mu\text{m} \cdot \text{cm} \cdot \text{V}^{-1} \cdot \text{sec}^{-1}$ at pH 8.0, $I = 100$ mM, 0 °C was used for calculation with Equation 2 (which is not strictly applicable at high ionic strength). The discrepancies claimed in ref.^[40] are mostly due to a wrongly quoted titration curve; since their $pI = 4.6$ at 0 °C matches to $pI = 4.7$ at 25 °C rather than with $pI = 4.9$, there nonetheless remains some 15% discrepancy with titration.

net charge Q at pH 8.0, 25 °C (titration) = -16 ± 2 ; from ref.^[41] adjusted to the more widely accepted $pI = 4.7$ (instead of $pI = 4.9$) which is corroborated by comparison with β -lactoglobulin in electrophoretic titration^[42] and also consistent with the protein sequence including two phosphoserines. At pH 8.0 the net charge is ionic strength insensitive.^[41]

$pI = 4.7$; at 25 °C,^[38] the pI increases with increasing ionic strength.

Stokes radius (R_s/nm) = 2.96; from critically selected sedimentation coefficients^[43,44] together with a sequence molecular weight of 44310 including carbohydrate plus two phosphates groups extra^[39] and a partial specific volume of 0.748 mL g⁻¹.

β -lactoglobulin:

This protein is a monomer below pH 3.0 and a dimer above pH 3.7;^[45] it denatures above pH 9.4.^[46] The dimer exists in 3 distinct conformations with transitions at pH 5.1^[43,47,48] and at pH 7–7.5.^[45,49,50]

net charge Q at pH 8.0, 25 °C (electrophoretic) = -15 ± 2 ; based on a mobility of $-1.7 \pm 0.1 \mu\text{m} \cdot \text{cm} \cdot \text{V}^{-1} \cdot \text{sec}^{-1}$ at pH 8.0, $I = 20 \text{ mM}$, 20 °C^[47,51] and calculated with Equation (2). The discrepancies claimed in ref. ^[51] are entirely explained by their neglect of Henry's function, a wrong molecular weight, the choice of pI , and a wrong Stokes radius.

net charge Q at pH 8.0, 25 °C (titration) = -15 ± 2 ; at $I = 10 \text{ mM}$, mean value of ref.^[45,46,49,51] based on a molecular mass of 36800 and including adjustments for ionic strength dependent variation of pI .^[46,50]

$pI = 5.2$ – 5.4 ; at 20 °C,^[38,46,50,51] the pI decreases with increasing ionic strength.

Stokes radius (R_s/nm) = 3.1 for the high pH dimer conformation;^[38,51] at pH 8.0 based on a diffusion coefficient and an s -value corrected for the Uppsala oil-turbine error.^[44]

Stokes radius (R_s/nm) = 2.89 ± 0.05 for the dimer below pH 7.0; based on diffusion coefficients^[47,52–55] and sedimentation coefficients^[43,56–58] in combination with a chain molecular mass of 18400,^[59] weight average sedimentation equilibrium of 37100^[47] and partial specific volume of 0.751 mL g⁻¹.^[47] In spite of reproducibly different s -values between low pH and neutral pH only an average Stokes radius can be given with statistical significance for the dimer below pH 7.0.

Acknowledgement: Support from NSF grant CHE-9021484 is gratefully acknowledged, as is assistance from Dr. Lars Hagel of Pharmacia Biotec.

Received: June 28, 1999

Revised: July 20, 2000

[1] W. W. Yau, J. J. Kirkland, D. D. Bly, "Modern Size Exclusion Chromatography", John Wiley and Sons, New York 1979.
 [2] C. F. Poole, S. K. Poole, "Chromatography Today", Elsevier, Amsterdam 1991.
 [3] E. F. Casassa, *J. Phys. Chem.* **1971**, 75, 3929.
 [4] T. C. Laurent, J. Killander, *J. Chromatogr.* **1964**, 14, 317.

[5] G. K. Ackers, *J. Biol. Chem.* **1967**, 242(13), 3237.
 [6] M. le Maire, A. Ghazi, M. Martin, F. Brochard, *J. Biochem.* **1988**, 106, 814.
 [7] P. L. Dubin, J. M. Principi, *Macromolecules* **1989**, 22, 1891.
 [8] P. L. Dubin, in: *Aqueous Size Exclusion Chromatography*; P. L. Dubin, Ed., Elsevier, Amsterdam 1988, Chapter 3.
 [9] M. Potschka, *J. Chromatogr.* **1988**, 441, 239.
 [10] B. Porsch, L. O. Sundeløf, *J. Chromatogr. A* **1994**, 669, 21.
 [11] M. G. Styring, C. J. Davison, C. Price, C. Booth, *J. Chem. Soc. Faraday Trans. 1*, **1984**, 80, 3051.
 [12] P. L. Dubin, M. M. Tecklenburg, *Anal. Chem.* **1985**, 57, 275.
 [13] P. L. Dubin, C. M. Speck, *Am. Chem. Soc. Div. Poly. Materials Sci. & Eng.* **1986**, 54, 194.
 [14] F. G. Smith III, W. M. Deen, *J. Colloid Interface Sci.* **1983**, 91, 571.
 [15] P. L. Dubin, R. M. Larter, C. J. Wu, J. I. Kaplan, *J. Phys. Chem.* **1990**, 94, 7243.
 [16] G. Shah, P. L. Dubin, J. I. Kaplan, G. R. Newkome, C. N. Morrefield, G. R. Baker, *J. Colloid Interface Sci.* **1996**, 183, 397.
 [17] M. Potschka, "A soft-body theory of size exclusion chromatography" in: *Strategies in Size Exclusion Chromatography*; M. Potschka, P. L. Dubin, Eds., ACS Symposium Series 635, American Chemical Society, Washington 1996, p. 67.
 [18] M. Potschka, *Macromolecules* **1991**, 24, 5023.
 [19] M. Potschka, *J. Chromatogr.* **1991**, 587, 276.
 [20] M. G. Davidson, W. M. Deen, *Macromolecules* **1988**, 21, 3474.
 [21] P. N. Lavrenko, O. I. Mikryukova, S. A. Didenko, *Polym. Sci. USSR* **1986**, 28, 576.
 [22] K. Luby-Phelps, P. E. Castle, D. L. Taylor, F. Lanni, *Proc. Natl. Sci. USA* **1987**, 84, 4910.
 [23] M. P. Bohrer, G. D. Patterson, P. J. Carrol, *Macromolecules* **1984**, 17, 1170.
 [24] L. Sachs, "Angewandte Statistik", 7th revised edition, Springer, Berlin 1992.
 [25] D. D. Perrin, B. Dempsey, "Buffers for pH and Metal Ion Control", Chapman & Hall, London 1974.
 [26] R. Pecora, B. J. Berne, "Dynamic Light Scattering", Wiley, New York 1976.
 [27] B. R. Ware, D. D. Haas, in: *Fast Methods in Physical Biochemistry and Cell Biology*, R. I. Shaafi, S. M. Fernandez, Eds., Elsevier, Amsterdam 1983.
 [28] R. J. Hunter, "Zeta potential in Colloid Science", Academic Press, New York 1988, p. 30.
 [29] D. J. Shaw, "Electrophoresis", Academic Press, New York 1969, p. 25.
 [30] C. Tanford, "Physical Chemistry of Macromolecules", Wiley, New York 1961; p. 416.
 [31] S. Hussain, M. S. Mehta, J. T. Kaplan, P. L. Dubin, *Anal. Chem.* **1991**, 63, 1132.
 [32] S. L. Edwards, thesis, Purdue Univ., 1992.
 [33] C.-H. Cai, V. Romano, P. L. Dubin, *J. Chromatogr. A* **1995**, 693, 251.
 [34] P. J. Flory, "Principles of Polymer Chemistry", Cornell Univ. Press, Ithaca NY 1953, p. 606.
 [35] R. H. Boyd, R. R. Chance, G. Ver Strate, *Macromolecules* **1996**, 29, 1190.
 [36] S. J. Shire, G. I. H. Hanania, F. R. G. Gurd, *Biochem.* **1974**, 13, 2967.
 [37] L. H. M. Janssen, S. H. De Bruin, G. A. J. Van Os, *Int. J. Peptide Res.* **1972**, 4, 339.
 [38] P. G. Righetti, T. Caravaggio, *J. Chromatogr.* **1976**, 127, 1.

- [39] R. Nave, K. Weber, M. Potschka, *J. Chromatogr.* **1993**, 654, 229.
- [40] L. G. Longworth, *Ann. N.Y. Acad. Sci.* **1941**, 41, 267.
- [41] R. K. Cannan, A. Kibrick, A. H. Palmer, *Annals N.Y. Acad. Sci.* **1941**, 41, 243.
- [42] L. A. Haff, L. G. Fägerstam, A. R. Barry, *J. Chromatogr.* **1983**, 266, 409.
- [43] G. L. Miller, R. H. Bolder, *Arch. Biochem. Biophys.* **1952**, 36, 249.
- [44] J. F. Taylor, *Arch. Biochem. Biophys.* **1952**, 36, 357.
- [45] M. Nagasawa, A. Holtzer, *J. Am. Chem. Soc.* **1971**, 93, 605.
- [46] Y. Nozaki, L. G. Bunville, C. Tanford, *J. Am. Chem. Soc.* **1959**, 81, 5523.
- [47] K. O. Pedersen, *Biochem. J.* **1936**, 30, 961.
- [48] K. Nitta, S. Sugai, *Biopolymers* **1972**, 11, 1893.
- [49] C. Tanford, L. G. Bunville, Y. Nozaki, *J. Am. Chem. Soc.* **1959**, 81, 4032.
- [50] M. Nagasawa, I. Noda, *J. Am. Chem. Soc.* **1968**, 90, 7200.
- [51] R. K. Cannan, A. H. Palmer, A. C. Kibrick, *J. Biol. Chem.* **1942**, 142, 803.
- [52] A. Polson, Thesis, U. of Stellenbosch 1937.
- [53] A. G. Ogston, *Proc. Roy. Soc. A (London)* **1949**, 196, 272.
- [54] J. M. Creeth, *J. Phys. Chem.* **1958**, 62, 66.
- [55] O. Lamm, A. Polson, *Biochem. J.* **1936**, 30, 528.
- [56] R. Cecil, A. G. Ogston, *Biochem. J.* **1948**, 43, 592.
- [57] M. le Maire, L. P. Aggerbeck, C. Monteilhet, J. P. Andersen, J. V. Møller, *Anal. Biochem.* **1986**, 154, 525.
- [58] A. G. Ogston, J. M. A. Tilley, *Biochem. J.* **1955**, 59, 644.
- [59] C. Tanford, K. Kawahara, S. Lapanje, *J. Am. Chem. Soc.* **1967**, 89, 729.
- [60] V. A. Romano, T. Ebeyer, P. L. Dubin, "Influence of net protein charge and stationary phase charge on protein retention in size exclusion chromatography" in: *Strategies in Size Exclusion Chromatography*, M. Potschka, P. L. Dubin, Eds., ACS Symposium Series 635, American Chemical Society, Washington 1996, p. 88.
- [61] H. Ohshima, T. W. Healy, L. R. White, *J. Colloid Interface Sci.* **1982**, 90, 17.
- [62] V. A. Parsegian, D. C. Rau, *J. Cell Biology* **1984**, 99, 196s.
- [63] J. N. Israelachvili, "Intermolecular and Surface Forces", Academic Press, London 1985.
- [64] M. Potschka, *Macromol. Symp.* **1996**, 110, 121.
- [65] L. Hagel, *J. Chromatogr.* **1993**, 648, 19.
- [66] L. Andersson, *J. Chromatogr.* **1981**, 216, 35.
- [67] H. Schrenker, *Amer. Lab.* **1978**, 10(5), 91.